Cross-sectional and plan-view cathodoluminescence of GaN partially coalesced above a nanocolumn array

K. J. Lethy,[1] P. R. Edwards,[1] C. Liu,[2] W. N. Wang,[2] and R. W. Martin[1,a)]
[1]*Department of Physics, SUPA, University of Strathclyde, Glasgow G4 0NG, United Kingdom*
[2]*Department of Electronic and Electrical Engineering, University of Bath, Bath BA2 7AY, United Kingdom*

(Received 22 November 2011; accepted 16 June 2012; published online 19 July 2012)

The optical properties of GaN layers coalesced above an array of nanocolumns have important consequences for advanced optoelectronic devices. GaN nanocolumns coalesced using a nanoscale epitaxial overgrowth technique have been investigated by high resolution cathodoluminescence (CL) hyperspectral imaging. Plan-view microscopy reveals partially coalesced GaN layers with a sub-μm scale domain structure and distinct grain boundaries, which is mapped using CL spectroscopy showing high strain at the grain boundaries. Cross-sectional areas spanning the partially coalesced GaN and underlying nanocolumns are mapped using CL, revealing that the GaN bandedge peak shifts by about 25 meV across the partially coalesced layer of $\sim$2 μm thick. The GaN above the nanocolumns remains under tensile strain, probably due to Si out-diffusion from the mask or substrate. The cross-sectional data show how this strain is reduced towards the surface of the partially coalesced layer, possibly due to misalignment between adjacent partially coalesced regions. © *2012 American Institute of Physics*. [http://dx.doi.org/10.1063/1.4737418]

I. INTRODUCTION

The growth of GaN on Si substrates is of significant interest because of the potential for use of large area substrates and integration with electronic devices along with advantages such as low cost, wide availability, and high thermal conductivity.[1,2] GaN-on-sapphire and GaN-on-SiC are currently the leading combinations for commercial high brightness blue/green/white light-emitting diodes (LEDs) and III-nitride wireless/RF products. GaN-on-silicon has yet to really make its mark on either of these industries but is the most promising material combination for achieving high device performance from growth on a low cost, large diameter platform. However, the growth of high quality GaN on Si is challenged by the large lattice (17%) and thermal expansion coefficient (56%) mismatches, which result in high densities of threading dislocations (TDs) and tensile stress in GaN epilayers on Si. GaN substrates with fewer threading dislocations are highly desirable for fabricating high-performance III-nitride devices and also for next generation laser diodes (LDs). Growth processes utilizing epitaxial lateral overgrowth (ELO) have proved significant in reducing dislocation densities and improving optical and electrical properties.[3] ELO reduces the density of threading dislocations by two mechanisms, namely, direct dislocation blocking and dislocation bending. However, TD densities $<10^{-6}\,cm^{-2}$ have so far not been achieved using this technique, and high performance devices are fabricated only on the ELO "wings." In addition, this technique results in strained (tensile or compressed) GaN layers.[4]It is the size of the "seed" regions (typically micron scale) that place a limit on the improvement that can be achieved using the ELO technique.[5–7]

Nano-ELO involving lateral overgrowth at the nanometer scale has been developed to overcome the limitations of the conventional ELO techniques and to reduce the dislocation density to below $10^{-6}\,cm^{-2}$, without the need to grow exceptionally thick (10 s–100 s of μm) layers of GaN. Nano-ELO limits the strained volume to extremely small areas and reduces the elastic deformation energy in the epitaxial film by providing nanometer sized relaxed seeds and thereby reducing the density of TDs.[8–11] Nano-ELO based on nanocolumns was first described by Luryi and Suhir.[10] GaN nanocolumns are one dimensional columnar nanostructures with high crystal quality and can possess improved optical properties due to their dislocation-free nature.[12] If the tops of such relaxed and dislocation-free GaN nanocolumns are coalesced by lateral growth, a GaN epitaxial layer with potentially little or no stress and very few dislocations can be obtained.

Three approaches have so far been reported for the coalescence of GaN nanocolumns: (a) an all molecular beam epitaxy (MBE) route, involving coalescence overgrowth of MBE grown GaN nanocolumns by switching from N-rich to Ga-rich conditions;[13] (b) an all metal organic vapour phase epitaxy (MOVPE) route,[9] involving coalescence overgrowth of GaN nanocolumns fabricated using a nano-imprint lithographic patterning;[11] and (c) growth of GaN nanocolumns by MBE followed by an MOVPE overgrowth.[8] In the present work, we report the optical properties of partially coalesced GaN nanocolumns obtained using the third approach on a Si substrate. Self-assembled GaN nanocolumns are produced by MBE on a Si [111] substrate, and then serve as seeds for nano-ELO by MOVPE. The optical properties of the partially coalesced GaN layers are investigated using high spatial resolution cathodoluminescence hyperspectral imaging to provide visualisation of the microstructure, information on the local luminescence and tracking of the strain variation across the partially coalesced layers. Collecting such data from cross-sections provides information as a function of depth within the grown layers.

a)E-mail: r.w.martin@strath.ac.uk.

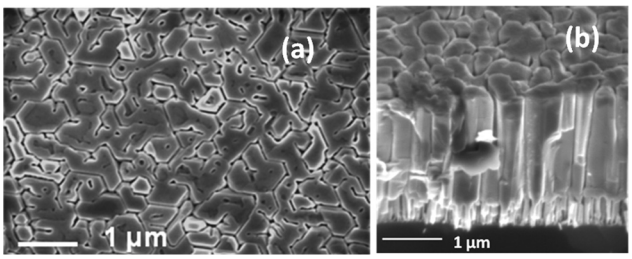

FIG. 1. (a) Plan-view and (b) cross-sectional SEM images of the partially coalesced GaN nanocolumns.

II. EXPERIMENTAL PROCEDURE

Growth of GaN nanocolumns on Si was carried out in an RF-MBE system having two Ga sources configured with different angles towards the growth substrate. NH_3 was used as the nitrogen source to grow layers of GaN and AlN. Prior to growth, the Si (111) substrate was heated to 950 °C for 60 min for thermal cleaning, followed by a 60 min surface nitridation at 1023 °C. The AlN buffer was deposited for 30 min at 850 °C. The substrate temperature was then raised to 900 °C, and the GaN nanocolumn structures were grown for 2 h using the two Ga sources.

Coalescence of the GaN nanocolumns was conducted in an Aixtron 200/4HT RF-S MOVPE reactor. The combined conventional growth mode, i.e., when gallium and nitrogen precursors are switched into the growth chamber simultaneously, and pulsed growth mode were applied.[14] Under the conventional growth mode, a growth temperature of 1150 °C, reactor pressure 100 mbar, V/III ratio in the range of 500–10 000, and the growth time corresponding to nominal planar growth for 2 μm GaN were used. The pulsed growth was employed to achieve the fast lateral growth in the early stage of coalescence. H_2 was used as the carrier gas in all the growth experiments.

The surface and cross-sectional morphology of the partially coalesced nanocolumns were studied by field emission gun scanning electron microscopy (FESEM), using an FEI Sirion 200. The light emitting properties were investigated by spatially and spectrally resolved room temperature cathodoluminescence (CL) set-ups attached to two different electron microscopy systems. High spatial resolution CL maps were collected from an angled sample using the FESEM (Ref. 15) and lower spatial resolution CL maps were obtained in plan-view using the CL set-up attached to a Cameca SX100 electron probe micro-analyser (EPMA).[4] Both these set-ups are capable of obtaining CL hyperspectral images, simultaneously mapping the spectral and spatial information. The application of appropriate mathematical methods to these three dimensional data set (λ, x, y) is used to extract the spatial distribution of peak intensity, peak energy and FWHM across the mapped region.

III. RESULTS AND DISCUSSION

The plan-view secondary electron image [Figure 1(a)] of the top GaN layer reveals that the surface of the overgrown epilayer is not continuous, but rather constituted by a number of sub-μm scale domain structures with distinct grain boundaries. The misalignment of adjacent GaN nanocolumns with respect to each other can possibly account for this incomplete coalescence with distinct grain boundaries. The cross-section SEM image, in Figure 1(b), shows the layer of GaN nanocolumns, approximately 500 nm in height,

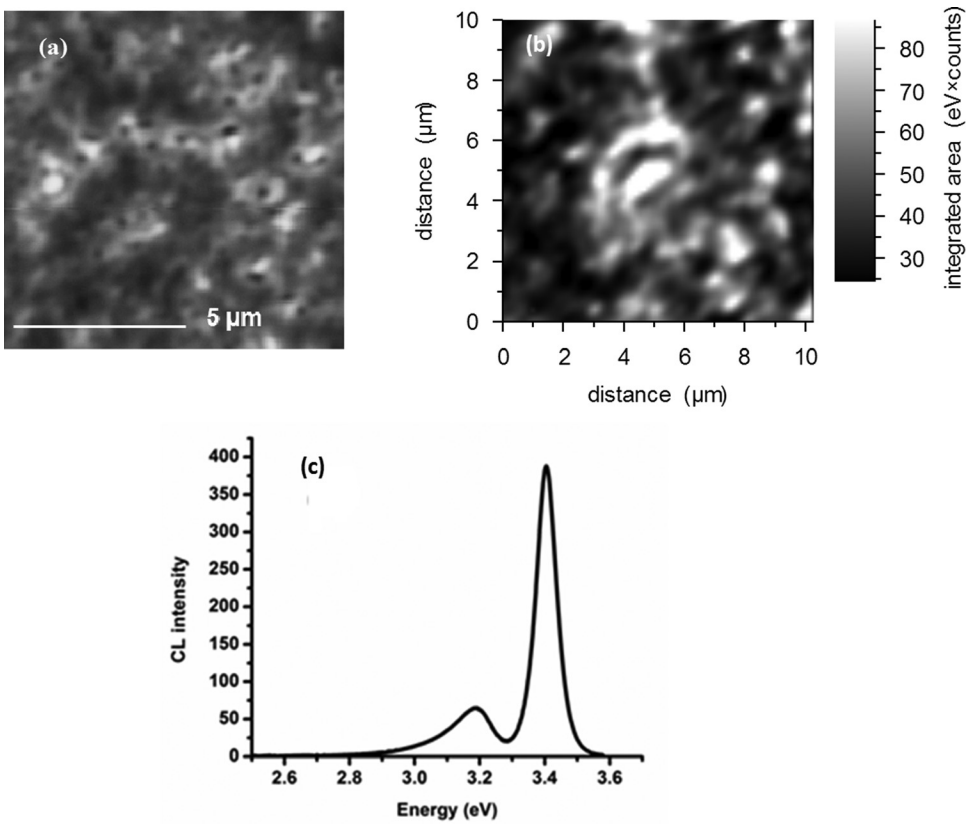

FIG. 2. (a) Secondary electron image of the partially coalesced GaN layer, (b) plan-view integrated intensity CL map from the partially coalesced GaN nanocolumns layer, (c) mean CL spectrum from the mapped region.

which then merge into larger columns giving an overgrown layer of partially coalesced GaN, about 2 μm in thickness.

A plan-view integrated intensity CL map from the partially coalesced nanocolumns acquired with an acceleration voltage of 10 kV using the CL setup attached to the EPMA is shown in Figure 2. The penetration depth (the depth at which the energy density of the incident electron beam has reduced by 90%) estimated using a Monte-Carlo simulation is ~370 nm for this accelerating voltage and is thus confined well within the partially coalesced layer. The CL emission intensity is not uniform across the partially coalesced layer and shows strong contrast between dark and bright regions. Figure 2(c) shows the mean CL spectrum for the mapped region in Figure 2(a) and presents two peaks at 3.41 eV and 3.19 eV. The 3.41 eV peak corresponds to GaN near band edge (NBE) emission and indicates a slight tensile strain in the partially coalesced GaN layer, by comparison with the NBE of bulk unstrained wurtzite GaN bandedge emission of 3.42 eV.[16] The peak appearing at 3.19 eV is most likely related to donor-acceptor pair (DAP) recombination. The most common donor species in GaN are O and Si, behaving as shallow donors. Although oxygen is not a usual contaminant in MBE growth, Si contamination is possible when using a Si substrate and Si-based mask material. In both MOVPE and MBE techniques, carbon is the most common residual acceptor contaminant.[12] However, since the GaN nanocolumn growth occurs under nitrogen rich conditions, the formation of Ga vacancies acting as acceptors is also likely.

Gaussian peak fitting to the individual CL spectra from each pixel, using a non-linear least squares (NLLS) algorithm, is used to generate maps showing the spatial distribution of peak height, center energy and FWHM for both GaN near band edge emission and the DAP emission, as shown in Figure (3). The CL intensity maps [Figures 3(a) and 3(d)] show the spatial intensity distribution of the NBE and DAP emission, respectively. Both are localized and randomly distributed and, importantly, these variations occur on a length scale much larger than that of the nanocolumn array. The spatial distribution of the DAP emission intensity indicates an inhomogeneous distribution of impurities across the partially coalesced surface, and it is noteworthy that there is a contrast difference between the domain center and boundaries.

The GaN NBE center energy CL map [Figure 3(b)] reveals micron-scale domain-like variations in peak energy, which can be attributed to the effects of the micron sized domain structures seen in the plan-view SEM. The effects of strain and/or doping can have a contribution to this variation in NBE CL emission. The thickening of GaN nanocolumns occurs by the merging of neighbors during the MOVPE overgrowth process and, together with minor misalignments

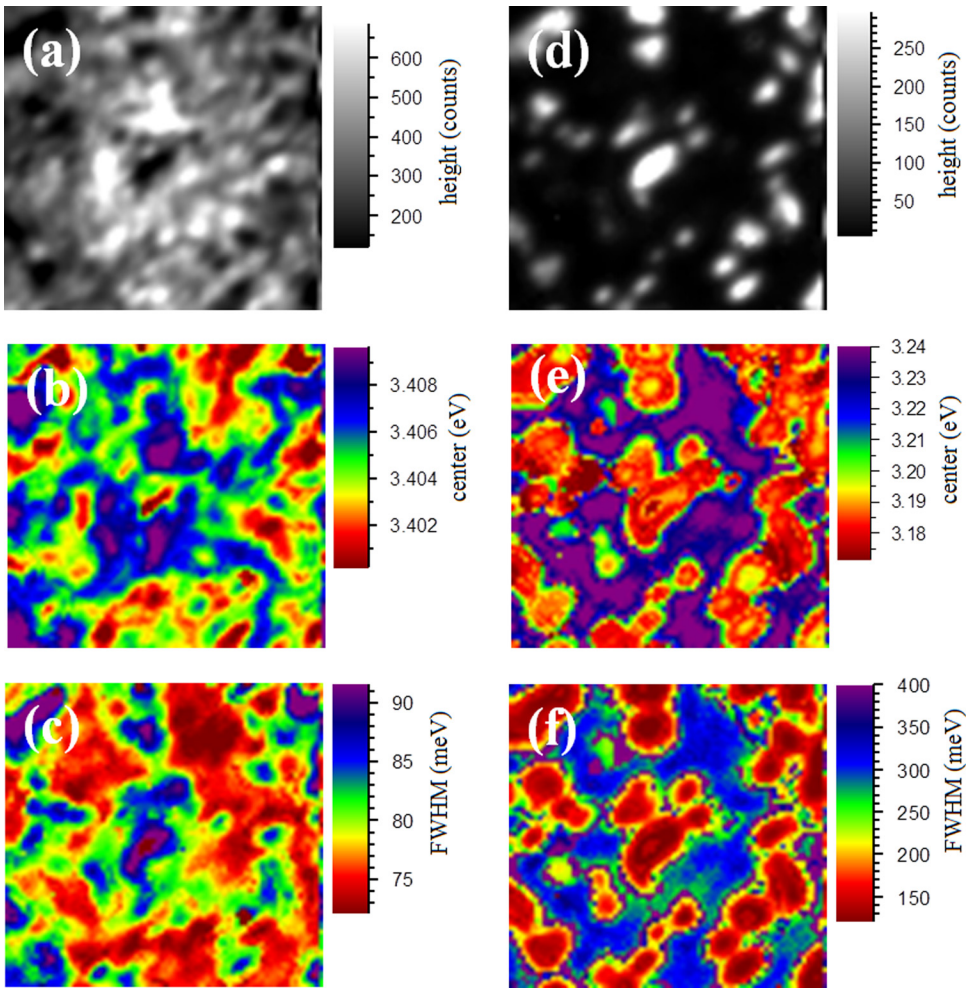

FIG. 3. The CL maps showing the distribution of peak intensity, center energy, and line width for the bandedge (a, b, and c, respectively) and DAP emission (d, e, and f, respectively).

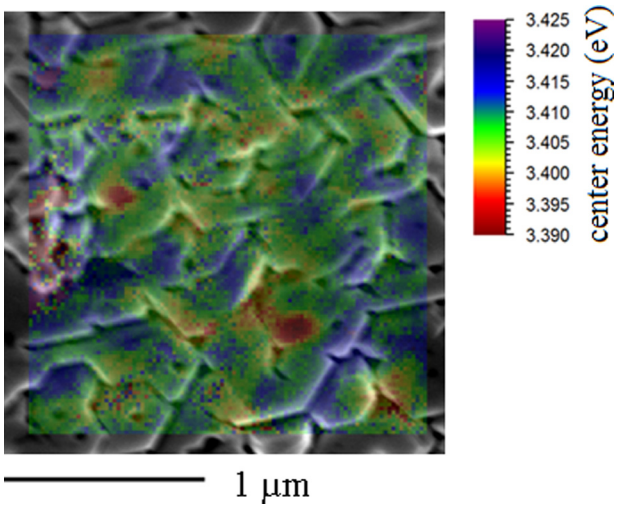

FIG. 4. The CL peak energy map of GaN NBE emission overlaid on the corresponding secondary electron image.

between the adjacent coalesced regions, can cause strain in the partially coalesced layer. CL maps taken at different electron beam energies, to provide some depth resolution, indicate that there is no significant variation in domain pattern with depth, for either intensity contrast or peak energy. The CL maps showing the spatial distribution of GaN NBE and DAP emission peak FWHM [Figs. 3(c) and 3(f)] also reveal μm scale range variations similar to those of the intensity and peak energy distributions.

To study the spatial distribution of strain across the partially coalesced GaN layer, high resolution plan-view CL hyperspectral maps are acquired from a $2 \times 2\ \mu m^2$ area of the sample using the FESEM CL set up. Figure 4 shows the CL peak energy map of GaN NBE emission overlaid on the secondary electron image. The grain boundaries are generally seen to match the higher energy (blue) regions, indicating higher compressive strain at these points. The merging of adjacent crystal domains, arising from non-perfectly aligned nanocolumns can account for the strain at the grain boundaries.[17]

Figure 5(a) shows a secondary electron image of a cross-section, which was then mapped using CL hyperspectral

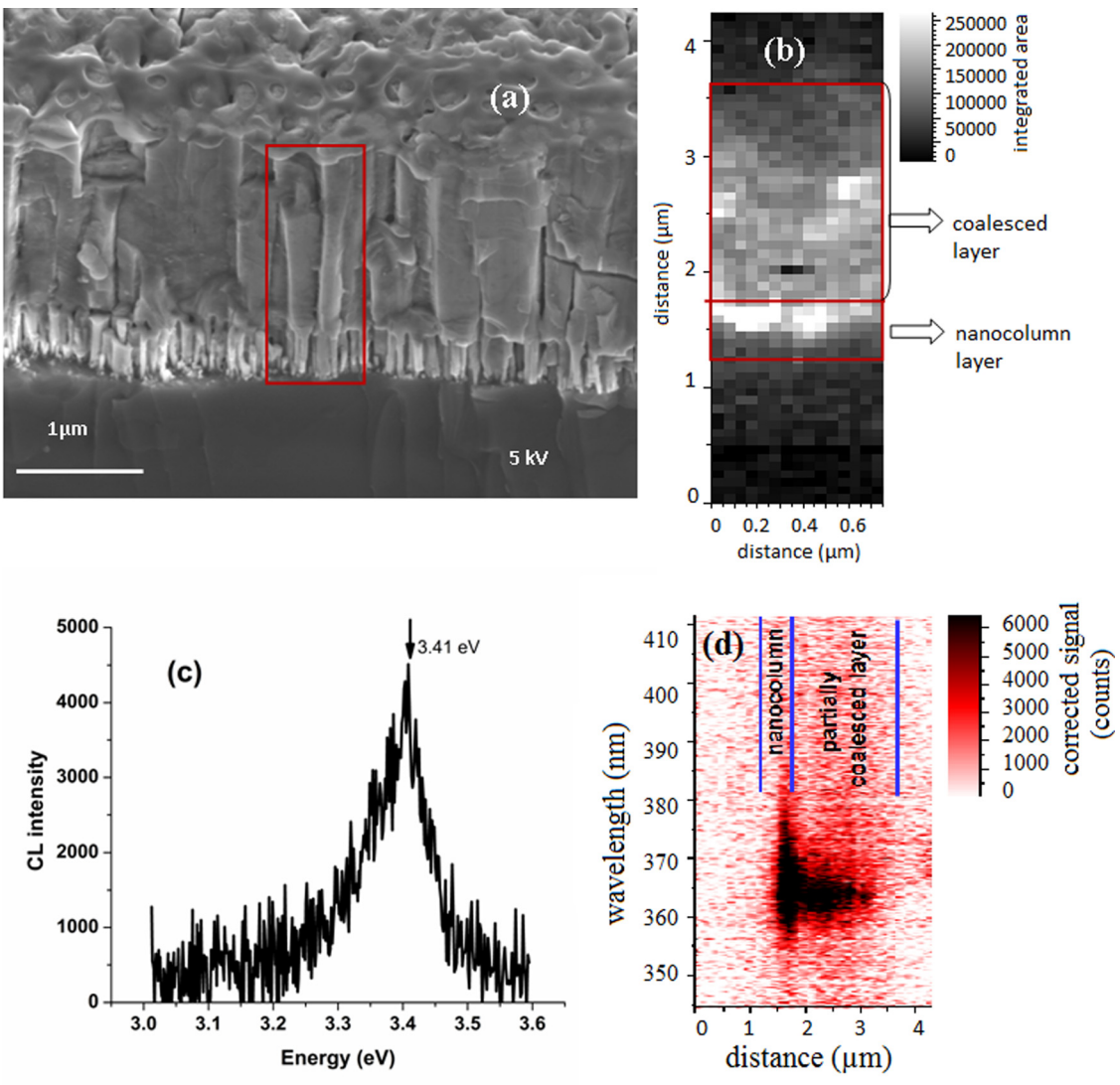

FIG. 5. (a) SE image showing the mapped region in a box, (b) cross-sectional CL integrated intensity map, (c) mean spectrum from the cross-section CL map, (d) line spectrum corresponding to CL line scan analysis.

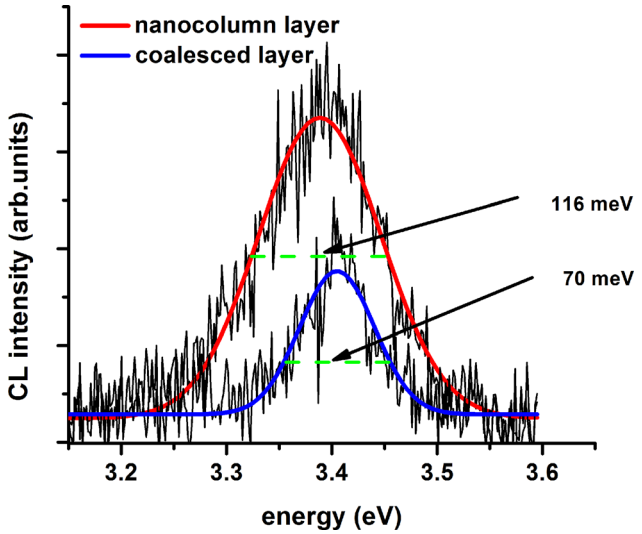

FIG. 6. Comparison of the spectra and FWHM of averaged line spectra from the nanocolumn layer and the top partially coalesced layer.

imaging in the FESEM. The mapped area was $1 \times 3\ \mu m^2$ with a step size of 100 nm and a dwell time of 500 ms per pixel. The mapped area is indicated by the box and includes both the partially coalesced and nanocolumn layers. Figure 5(b) shows the integrated intensity CL map across the cross-section with lines separating the emission from the partially coalesced and nanocolumn regions.

The CL emission is brighter from the nanocolumn layer relative to the partially coalesced layer indicating the higher optical quality of the nanocolumn layer which can be attributed to its lower dislocation density.[12,18] This can also be due to the improved light extraction efficiency of one dimensional nanocolumns. The dislocation density reduction in the nanocolumns is partially due to the dislocation bending in the nanocolumns and dislocation blocking effect of the SiO_2 mask and partially due to strain relaxation in the nanometer sized nucleation and growth.[19] A similar observation of brighter CL from the nanocolumn layer has been reported by Tang *et al.*[11] from samples fabricated using nano-imprint lithography and MOVPE, although the same authors have reported the opposite behaviour for coalescence above MBE nanocolumns grown from an AlN nucleation layer.[20]

The spectra from the full height of Figure 5(b), averaged across the 15 pixels of the map are plotted as a CL line scan in Fig. 5(d). The analysis of this cross-section map reveals a blue shift of ~25 meV in the GaN bandedge CL peak as the sampled region moves upward from the nanocolumn layer, through the partially coalesced layer of thickness ~2 μm. This shift in the GaN band-edge emission can be related to the release of tensile strain through the partially coalesced layer. This is in agreement with the observation by Shiao *et al.*[17] where the strain across an overgrown GaN layer of similar thickness decreases with an increase in thickness of the coalescence layer. Similarly, Tang *et al.*[11] observed a rebuilding of compressive strain (~0.66 GPa) in a GaN coalesced layer over strain free nanocolumns grown on nanopatterned sapphire substrate. Bougrioua *et al.*[8] also reported the incorporation of strain in an MOVPE overgrown GaN layer using PL spectroscopy, with coalescence started from strain-free nanopillars grown by MBE, although in this case the sense was tensile.

A comparison of the averaged CL spectra obtained from line scan analysis of 15 pixels across the nanocolumn layer and the top part of the partially coalesced layer reveals that the GaN bandedge emission from the nanocolumn layer is broader [Figure 6] (by approximately 50 meV) and more tensile strained than from the partially coalesced layer. The small dimensions of the nanocolumns allow for local strain relaxation, permitting the lattice parameter to approach its bulk value. Hence, the GaN nanocolumns are expected to grow strain-free and defect-free with a single hexagonal crystal structure, as has been experimentally observed by several research groups.[12,21] This leads to an expectation that the GaN layer structure realized by coalescence of these strain free nanocolumns should be completely strain relaxed. However, the tensile strain from the nanocolumn layer observed in the present case could be due to high residual doping. Liu *et al.*[22] also observed a tensile stress for micro-scale pyramid facets near the base of ELO GaN grown over a SiO_2 mask. Figure 7 clarifies how the blueshift and narrowing of the GaN bandedge emission develop as the electron beam scans from the nanocolumn layer to the top layers of partially coalesced overgrowth GaN. Each data point on these plots is obtained by Gaussian peak fitting to the

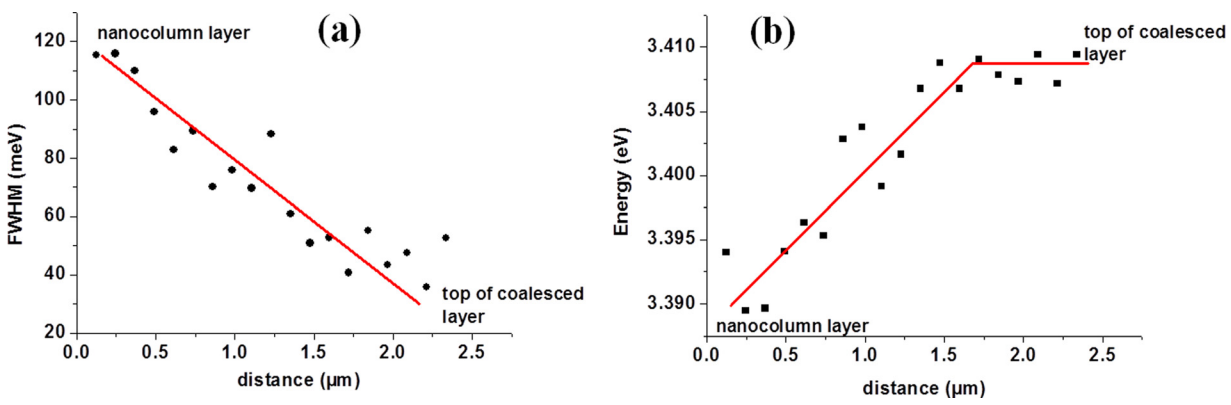

FIG. 7. (a) FWHM and (b) wavelength variation of the NBE emission as the electron beam scans from the nanocolumn layer to the top of the partially coalesced layer. The lines are guides to the eye.

individual CL spectra, averaged across 15 pixels on a line spectrum.

The tensile strain from doping arises due to Si from the substrate or mask diffusing to the nanocolumn layer. Substitution of Si in place of Ga in the GaN lattice results in a net contraction of the lattice as the Si atoms (~100 pm) are smaller than the Ga atoms (130 pm). Dadgar *et al.*[23] and Lee *et al.*[24] have previously reported tensile strain in Si doped GaN layers. The FWHM analysis of the PL spectra for bandedge emission from GaN as a function of Si doping by Schubert *et al.*[25] and Lee *et al.*[26] revealed an increase in FWHM of the bandedge emission with increase in Si doping concentration. Tang *et al.*[11] also observed a similar broadening effect for the GaN bandedge emission from regularly patterned GaN nanocolumns on sapphire substrate. However, the nanocolumns in the present case are not uniformly patterned or well ordered arrays as reported by Tang *et al.* The MBE grown nanocolumns have slight dispersions in their height, width, and orientation, as shown in Figure 1, which can contribute to the broadening of the FWHM of the GaN bandedge emission.

The peak of the mean band edge CL emission (~3.41 eV) from the plan view map is comparable to that collected from the top partially coalesced layers in the cross-sectional CL map (~3.41 eV), but shifted from that of unstrained bulk GaN emission (3.42 eV) implying that the partially coalesced layer is not fully relaxed and under a slight tensile strain. The absence of a continuous crystal surface and the presence of distinct domain structure as seen in the SEM image, and a possible epitaxial misalignment due to random orientation of the growth facets between adjacent domains as suggested by the plan view CL map, can result in a build up of compressive strain in the GaN overgrown layer, reducing the tensile strain.

Investigation of a similar region further along the cross-section revealed a slightly different strain situation. Starting from the top of the nanocolumns, a slight redshift of ~20 meV for GaN bandedge emission is observed across the partially coalesced GaN layer, indicating a build up of tensile strain as the coalescence overgrowth proceeds. Analysis of individual CL spectra averaged across 15 pixels obtained from line scan analysis along the partially coalesced layer further revealed that the initial layers of the overgrowth layer are tensile strain relaxed.

It is worth mentioning that the mean CL spectrum collected from some regions of the cross-section has a shoulder emission at 3.35 eV in addition to the bandedge emission peak. There are two different views about the origin of this peak. Bunea *et al.*[27] attributed this shoulder emission to re-absorption where as Chen *et al.* reported this emission at 3.35 eV to be related to localized or extended defects, such as stacking faults and dislocations or shallow levels in the bandgap.[28] The presence of this shoulder emission peak in the coalesced overgrown GaN layer on sapphire and Si substrates is reported by Tang *et al.*[11,20] An intensity comparison of the emission at 3.35 eV to the NBE emission across the nanocolumn and partially coalesced layers was performed using the mean CL spectra collected from the respective layers. No consistent behaviour exists for the ratio $I_{3.35}/I_{NBE}$ across the nanocolumn layer and partially coalesced layer, implying that the defects, if they are the cause of this emission, are randomly distributed across the nanocolumn layer and partially coalesced layer.

IV. CONCLUSIONS

The optical properties of a GaN layer coalesced by MOVPE starting from MBE grown nanocolumns on Si substrate have been studied using CL hyperspectral imaging. The overgrown GaN layer is partially coalesced with distinct grain boundaries, with plan-view CL hyperspectral imaging revealing micron-scale domain-like spatial variations of the GaN NBE emission energy and FWHM. Higher resolution plan-view CL mapping indicated that the grain boundaries associated with this partially coalesced GaN are under strain. Cross-sectional CL hyperspectral imaging identified a blue shift of ~25 meV, and a narrowing of the GaN bandedge emission peak, as the electron beam sampled region moves upward from the nanocolumn layer. This energy shift is possibly associated with the release of tensile strain through the partially coalesced GaN layer.

ACKNOWLEDGMENTS

The authors would like to thank the Overseas Research Award Scheme (ORS) and EPSRC for financial support.

[1]F. Semond, Y. Cordier, N. Grandjean, F. Natali, B. Damilano, S. Vézian, and J. Massies, Phys. Status Solidi A **188**, 501 (2001).
[2]A. Krost and A. Dadgar, Phys. Status Solidi A **194**, 361 (2002).
[3]S. F. Chichibu *et al.*, Appl. Phys. Lett. **74**, 1460 (1999).
[4]R. W. Martin, P. R. Edwards, K. P. O'Donnell, M. D. Dawson, C. W. Jeon, C. Liu, G. R. Rice, and I. M. Watson, Phys. Status Solidi A **201**, 665 (2004).
[5]H. Marchand, X. H. Wu, J. P. Ibbetson *et al.*, Appl. Phys. Lett. **73**, 747 (1998).
[6]A. Sakai, H. Sunakawa, and A. Usui, Appl. Phys. Lett. **73**, 481 (1998).
[7]D. Kapolnek, S. Keller, R. Ventury, R. D. Underwood, P. Kozodoy, S. P. D. Baars, and U. K. Mishra, Appl. Phys. Lett. **71**, 1204 (1997).
[8]Z. Bougrioua, P. Gibart, E. Calleja, U. Jahn, A. Trampert, J. Ristic, M. Utrera, and G. Nataf, J. Cryst. Growth **309**, 113 (2007).
[9]L. S. Wang, S. Tripathy, B. Z. Wang, J. H. Teng, S. Y. Chow, and S. J. Chua, Appl. Phys. Lett. **89**, 011901 (2006).
[10]S. Luryi and E. Suhir, Appl. Phys. Lett. **49**, 140 (1986).
[11]T. Y. Tang *et al.*, J. Appl. Phys. **105**, 023501 (2009).
[12]E. Calleja, M. A. Sanchez-Garcia, F. J. Sanchez, F. B. Naranjo, E. Munoz, U. Jahn, and K. Ploog, Phys. Rev. B **62**, 16826 (2000).
[13]D. Cherns, L. Meshi, I. Griffiths, S. Khongphetsak, S. V. Novikov, N. Farley, R. P. Campion, and C. T. Foxton, Appl. Phys. Lett. **92**, 121902 (2008).
[14]C. Liu, P. A. Shields, S. Denchitcharoen, S. Stepanov, A. Gott, and W. N. Wang, J. Cryst. Growth **300**, 104 (2007).
[15]P. R. Edwards and R. W. Martin, Semicond. Sci. Technol. **26**, 064005 (2011).
[16]W. S. Lee *et al.*, Appl. Phys. Lett. **94**, 082105 (2009).
[17]W. Y. Shiao, T. Y. Tang, Y. S. Chen, K. L. Averett, J. D. Albrecht, and C. C. Yang, J. Cryst. Growth **310**, 3159 (2008).
[18]S. D. Hersee, X. Sun, and X. Wang, Nano Lett. **6**, 1808 (2006).
[19]Z. Keyan, W. Yadong, and C. S. Jin, Phys. Status Solidi C **6**, S514 (2009).
[20]T. K. Tang, K. L. Averett, J. D. Albrecht, W. Y. Shiao, Y. S. Chen, C. C. Yang, C. W. Hsu, and L. C. Chen, Nanotechnology **18**, 445601 (2007).
[21]L. Cerutti, J. Ristic, F. S. Garrido, E. Calleja, A. Trampert, K. H. Ploog, S. Lazic, and J. M. Calleja, Appl. Phys. Lett. **88**, 213114 (2006).
[22]Q. K. K. Liu, A. Hoffmann, H. Siegle, A. Kaschner, C. Thomsen, J. Christen, and F. Bertram, Appl. Phys. Lett. **74**, 3122 (1999).

[23]A. Dadgar, F. Schulze, T. Zettler, K. Haberland, R. Close, G. Straburger, J. Bläsing, A. Diez, and A. Krost, J. Cryst. Growth **272**, 72 (2004).
[24]I. H. Lee, I. H. Choi, C. R. Lee, E. Shin, D. Kim, S. K. Noh, S. J. Son, K. Y. Lim, and H. J. Lee, J. Appl. Phys. **83**, 5787 (1998).
[25]E. F. Schubert, I. D. Goepfert, and W. Grieshaber, Appl. Phys. Lett. **71**, 921 (1997).
[26]I. H. Lee, J. J. Lee, P. Kung, F. J. Sanchez, and M. Razeghi, Appl. Phys. Lett. **74**, 102 (1999).
[27]G. E. Bunea, W. D. Herzog, M. S. Unlu, B. B. Goldberg, and R. J. Molnar, Appl. Phys. Lett. **75**, 838 (1999).
[28]G. D. Chen, M. Smith, J. Y. Lin, H. X. Jiang, A. Salvador, B. N. Sverdlov, A. Botchkarv, and H. Morkoc, J. Appl. Phys. **79**, 2675 (1996).